SLAC-PUB-11900
July 2006

MONITORING OF INTERACTION-POINT PARAMETERS USING THE 3-DIMENSIONAL LUMINOSITY DISTRIBUTION MEASURED AT PEP-II*

B. F. Viaud†, Université de Montréal, Montréal, Québec, Canada H3C 3J7
W. Kozanecki, DAPNIA-SPP, CEA-Saclay, F91191 Gif-sur-Yvette, France
C. O'Grady, J. Thompson, M. Weaver, Stanford Linear Accelerator Center, Stanford CA 94309, U.S.A.

Abstract

The 3-D luminosity distribution at the IP of the SLAC B-Factory is monitored using $e^+e^- \to e^+e^-$, $\mu^+\mu^-$ events reconstructed online in the *BABAR* detector. The transverse centroid and spatial orientation of the luminosity ellipsoid reliably monitor IP orbit drifts. The longitudinal centroid is sensitive to small variations in the average relative RF phase of the beams and provides a detailed measurement of the phase transient along the bunch train. The longitudinal luminosity distribution depends on the $e^{+,-}$ overlap bunch length and the vertical IP β-functions. Relative variations in horizontal luminous size are detectable at the micron level. In addition to continuous on-line monitoring of all the parameters above, we performed detailed studies of their variation along the bunch train to investigate a temporary luminosity degradation. We also compare β_y^* measurements, collected over a year of high-luminosity operation, with HER and LER lattice functions measured by resonant transverse excitation. Our bunch-length measurements are consistent with those obtained by other methods and provide direct evidence for bunch-length modulation.

LUMINOUS-REGION MONITORING

When the PEP-II B-Factory [1] operates at a luminosity of $10^{34} cm^{-2} s^{-1}$, about 1500 $e^+e^- \to e^+e^-$, $\mu^+\mu^-$ events are reconstructed per minute in the *BABAR* detector [2]. The three-dimensional centroid and orientation of the luminous ellipsoid, determined from the spatial distribution of event vertices, are now routinely provided to the accelerator every five to ten minutes, as illustrated in Fig. 1 and more extensively documented in Ref. [3]. The horizontal tilt of the luminous region, $\langle x' \rangle_{\mathcal{L}} = \left\langle \frac{dx}{dz} \right\rangle_{\mathcal{L}}$, together with the average horizontal boost angle $\langle x'_{\rm B} \rangle$ of $\mu^+\mu^-$ pairs [4], provide an online measurement of the horizontal e^+e^- crossing angle. Also reported, on time scales varying from a few minutes to an hour depending on the observable, are the resolution-corrected horizontal luminous size $\sigma_{x\mathcal{L}}$ [3], the horizontal and vertical e^- angular divergence [4], as well as the longitudinal overlap beam size Σ_z, the vertical IP β function $\beta_y^{*,eff}$ and the effective optical waist z_y^{eff}, discussed below. Reconstructed physics events are also archived for offline studies seeking a more precise characterization of the luminous region.

* Work supported in part by DOE Contract DE-AC02-76SF00515
† viaud@slac.stanford.edu

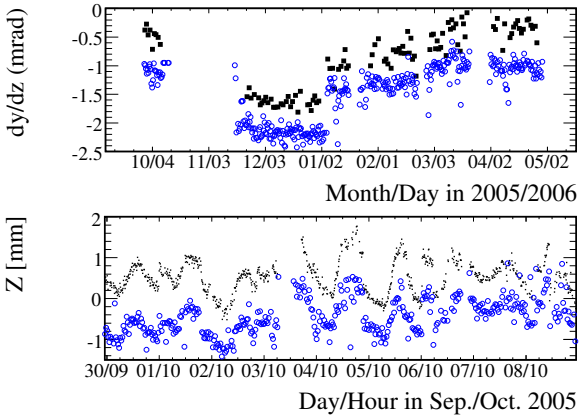

Figure 1: Top: History of the vertical luminous tilt $\langle y' \rangle_{\mathcal{L}}$ (black squares), and vertical e^- IP angle reported by the beam position monitor system (blue open circles). The steps reflect deliberate adjustments of the orbit after major accelerator maintenance. Bottom: history of the longitudinal luminous centroid (dots), and half of the differential RF phase between the two rings (blue open circles). The BPM and RF-phase data have arbitrary zero offsets.

β_y^* MEASUREMENTS

Neglecting dispersive and x-y coupling effects, the differential luminosity distribution $\mathcal{L}(z)$ is given by [5]:

$$\mathcal{L}(z) = \frac{2 f_c N_+ N_-}{\sqrt{(2\pi)^3}\Sigma_x \Sigma_y \Sigma_z}\, exp\left(\frac{-2(z-z_c)^2}{\Sigma_z^2}\right) \qquad (1)$$

where f_c is the collision frequency, z_c is the longitudinal position the bunch-crossing point, $N_{+,-}$ are the $e^{+,-}$ bunch populations, $\Sigma_z = \sqrt{\sigma_{z+}^2 + \sigma_{z-}^2}$, $\sigma_{z+,-}$ are the bunch lengths, and (with $t = x, y$)

$$\Sigma_t = \sqrt{\sigma_{t+}^{*2}\left(1 + \frac{(z-z_{t+})^2}{\beta_{t+}^{*\,2}}\right) + \sigma_{t-}^{*2}\left(1 + \frac{(z-z_{t-})^2}{\beta_{t-}^{*\,2}}\right)}$$

Here $\sigma_{ti}^* = \sqrt{\epsilon_{ti}\beta_{ti}^*}$ $(i = +, -)$ is the horizontal or vertical size of beam i at its waist z_{ti}; ϵ_{ti} and β_{ti}^* are, respectively, the corresponding emittance and the β function at the waist. The dominantly Gaussian shape of $\mathcal{L}(z)$ is modified, through its Σ_y dependence, by an hourglass factor

function of $\beta^*_{y+,-}$ (the β^*_x dependence is negligible). This can be expressed in terms of an effective β-function:

$$\beta_y^{*,eff} = \sqrt{\frac{\epsilon_{y-}\beta^*_{y-} + \epsilon_{y+}\beta^*_{y+}}{\epsilon_{y-}/\beta^*_{y-} + \epsilon_{y+}/\beta^*_{y+}}}$$

provided the two waists occur at the same location ($z_{y+} = z_{y-} = z_y^{eff}$).

Σ_z, $\beta_y^{*,eff}$, z_c and z_y^{eff} are extracted from a fit of Eq. 1 to the z-distribution of event vertices. Small distortions of this distribution by geometrical-acceptance effects were investigated using real data samples as well as a GEANT4 simulation that incorporates a complete description of the *BABAR* response, and eliminated by tightening the event selection. Two additional methods provide statistically independent information about the vertical IP β-functions during high-current operation. The longitudinal dependence of the vertical RMS boost angular spread $\sigma_{y'_B}$ [4] depends on $\beta^*_{y+,-}$ because the y-y' correlation intensifies as one moves away from the waist; it can be analyzed in terms of the same effective β-function as the longitudinal luminosity profile. The vertical luminous size $\sigma_{y\mathcal{L}}$ [6] increases as a function of the distance to the waist, at a rate that depends on $\beta^*_{y+,-}$ and $\epsilon^*_{y+,-}$, albeit with a slightly different functional dependence from that of $\beta_y^{*,eff}$ above. The instrumental systematics are of a different nature for the three techniques; they are estimated at $\Delta\beta^*_y \sim 3$ mm for the vertical luminous size and ~ 1 mm for the other two methods. The evolution of these β^*_y estimators and their comparison with a common set of lattice functions measured in single-bunch mode by resonant excitation, is compiled in Fig. 2.

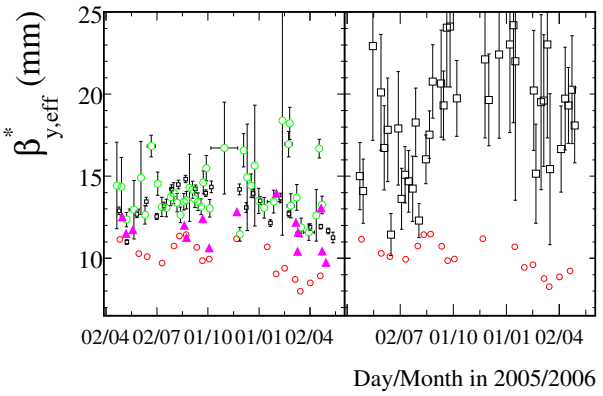

Figure 2: $\beta_y^{*,eff}$ determination, using the longitudinal luminosity profile (left, small squares), the RMS angular spread of the $\mu^+\mu^-$ boost vector (left, green circles with error bars), and the vertical luminous size (right, open black squares). The open red circles represent phase-advance measurements of $\beta^*_{y+,-}$, appropriately combined assuming $\epsilon_{y+} = \epsilon_{y-} = 3$ nm-rad. The purple triangles are the result of fits to $\mathcal{L}(z)$ distributions simulated using fully-coupled lattice functions.

The inconsistency in $\beta_y^{*,eff}$ between the luminous-region results and the vertical phase-advance measurements can be largely resolved by taking x-y coupling into account. Longitudinal luminosity distributions, simulated using the formalism of Ref. [7] and fully-coupled lattice functions measured using a "MIA" technique [8], were fitted using the uncoupled formalism of Eq. 1. The resulting $\beta_y^{*,eff}$ values lie closer to our luminous-region results. A similar, albeit preliminary study applied to the boost and vertical luminous size methods yields the same conclusion. In all cases however, the predicted value of $\beta_y^{*,eff}$ is somewhat sensitive to the smaller ($\sim$ vertical) e^+ and e^- eigenemittances that are assumed when combining measured HER and LER IP lattice functions. A fully self-consistent determination of IP beam parameters under high-luminosity conditions remains to be carried out.

VARIATION OF IP BEAM PARAMETERS ALONG THE BUNCH TRAIN

For several months in mid-2005, PEP-II observed a significant, systematic variation of the luminosity along the bunch train. This is illustrated in Fig. 3a, where the rate of reconstructed e^+e^-, $\mu^+\mu^-$ events is displayed as a function of where along the train the event occurred. The time stamp of the *BABAR* trigger relative to the accelerator turn signal locates an approximate bucket number; the more precise drift chamber information identifies the exact bucket to within $\sim 2ns$. The individual minitrains are clearly visible. The event rate, equivalent to the specific luminosity $\mathcal{L}_{sp}$ because the bunch currents are uniform within about 2% RMS, drops by $\sim$15% from the head to the tail of each minitrain.

Extensive studies were performed to understand these observations, which accounted for a $\sim$10% deficit in average luminosity. In the particular dataset presented here, the luminous z-centroid (Fig. 3b) varies by 5 mm peak-to-peak along the full train, reflecting the differential RF-phase transient between the e^+ and e^- rings. A 1- 2 mm variation occurs within each minitrain; geometrical considerations (that ignore beam-beam effects, if any) limit its predicted impact on $\mathcal{L}_{sp}$ to less than 2%. The most statistically significant signal is a 2 μm variation of $\sigma_{x\mathcal{L}}$ along the minitrain (Fig. 3c), which, depending on the e^+/e^- IP spot size ratios, might explain most of the luminosity drop. Unfortunately, the statistical precision of the vertical luminous-size (Fig. 3d), measured along the minitrain using the method of Ref. [6], remains insufficient to reveal any systematic degradation of the vertical IP spot size, as might be induced for instance by electron-cloud effects. Studies of variations in Σ_z or $\beta_y^{*,eff}$ along the train provide no additional clue. Empirical tuning ultimately eliminated most of the $\sigma_{x\mathcal{L}}$ and $\mathcal{L}_{sp}$ variation along the train.

BUNCH LENGTH MEASUREMENTS

Fig. 4 displays archived online measurements of Σ_z at different accelerating voltages, and compares them to the quadratic sum of the e^+ and e^- bunch lengths measured

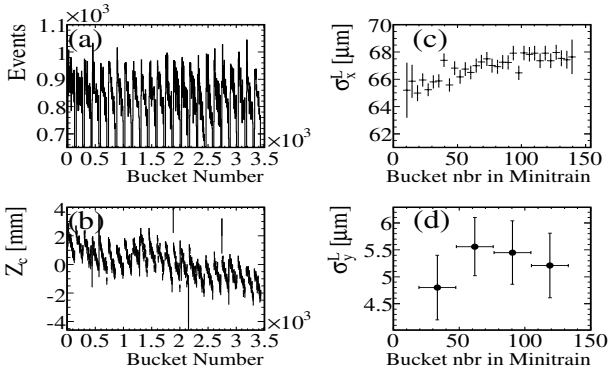

Figure 3: (a, b) Variation of the number of e^+e^-, $\mu^+\mu^-$ events and of the luminous z-centroid along the full bunch train. The abort gap occurs at the right edge of the plots. (c, d) Variation of the horizontal and vertical luminous size along one minitrain, averaged over all minitrains.

separately, at distant time intervals, by fitting the frequency spectrum at pickup electrodes in the HER and LER [10]. The two methods report comparable changes in luminous length, with a magnitude roughly consistent with the variations in accelerating voltage; the absolute length scales of the two sets of measurements agree within about 3%. However, the more frequent luminous-region measurements exhibit systematic variations, at apparently constant RF voltage, that (unlike the $\beta_y^{*,eff}$ results) cannot be explained by IP-coupling effects and remain to be understood.

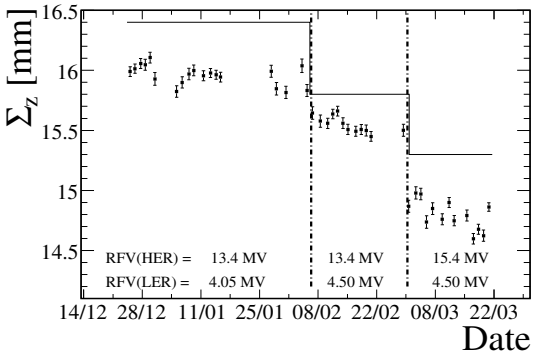

Figure 4: Σ_z measurements based on the longitudinal luminosity profile (points with statistical error bars), and computed from bunch length measurements in the two rings by a spectral method (solid lines) at various gap voltages.

The technique of the preceding section can be extended to measure bunch length modulation. The variation, along the bunch train, of Σ_z^2 and z-centroid, are compared in Fig. 5 to an analytical prediction [9] of Σ_z^{RF} (computed from the individual e^+ and e^- bunch-length predictions) and of the differential RF-phase transient. This prediction takes into account the actual bunch pattern, bunch currents and RF complement to compute, in each ring separately, the expected RF loading, phase transient, RF-voltage and bunch-length variation along the train. The predicted amplitude and phase of the bunch-length modulation and phase transient are in satisfactory agreement with our measurement. Because the RF model yields only the zero-current bunch lengths, its predictions remain to be corrected for impedance-induced bunch lengthening, which is expected to remain approximately constant along the train.

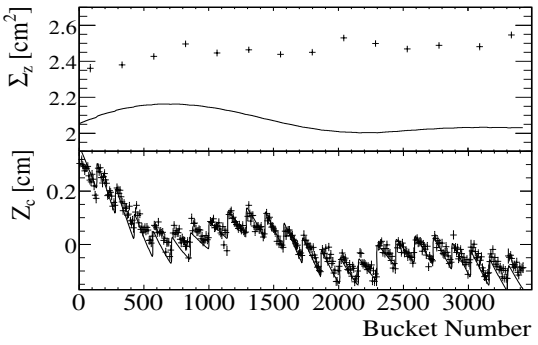

Figure 5: Bunch-number dependence of Σ_z^2 (top) and z-centroid (bottom) along a full train. Luminous-region data (points with error bars) are compared to the analytical prediction of an RF model at zero beam current (solid line).

CONCLUSION

Online monitoring of the colliding-beam phase space at the PEP-II IP using *BABAR* data, has been significantly improved by combining information from the 3-D luminosity distribution with that provided by the transverse boost of muon pairs. The longitudinal observables (collision-phase transient, overlap bunch length) are instrumentally robust, insensitive to transverse phase-space assumptions, and in agreement with more traditional techniques. Measurements of the effective vertical IP β function by three independent methods yield mutually consistent results, that can be reconciled with BPM-based lattice characterization data by taking IP coupling effects into account.

REFERENCES

[1] J. Seeman *et al.*, EPAC-2006-MOPLS045.

[2] B. Aubert *et al.* [*BABAR* Collaboration], Nucl. Instrum. Meth. A **479**, 1 (2002).

[3] B. Viaud *et al.*, SLAC-PUB-11682.

[4] M. Weaver *et al.*, SLAC-PUB-11906.

[5] M. Venturini and W. Kozanecki, SLAC-PUB-8699.

[6] J. M. Thompson *et al.*, SLAC-PUB-11222.

[7] Y. Cai, SLAC-PUB-8479; W. Colocho, private communication.

[8] Y. T. Yan *et al.*, SLAC-PUB-9368 and PAC-2005-MPPE059; Y. Cai *et al.*, EPAC-2006-MOPLS052.

[9] D. Teytelman, SLAC-PUB in preparation.

[10] A. Fisher *et al.*, PAC-2005-TPPP026.